

Comparison of Magnetic and Electrical Properties in Amorphous, Quasicrystalline and Crystalline States of Al-Mn Alloys

著者	Fukamichi Kazuaki, Goto Tsuneaki
journal or publication title	Science reports of the Research Institutes, Tohoku University. Ser. A, Physics, chemistry and metallurgy
volume	34
number	2
page range	267-287
year	1989-03-20
URL	http://hdl.handle.net/10097/28322

Comparison of Magnetic and Electrical Properties in Amorphous,
Quasicrystalline and Crystalline States of Al-Mn Alloys*

Kazuaki Fukamichi** and Tsuneaki Goto***,

Department of Materials Science, Faculty of Engineering, Tohoku University
(Received January 6, 1989)

Synopsis

The magnetic and electrical properties in the amorphous, quasicrystalline and crystalline states of Al-Mn and Al-Mn-Si alloys have been investigated and compared because the amorphous structure is often correlated with the icosahedral structure, and the structures of some crystalline compounds are resemble to that of the quasicrystalline alloys. The magnetizations measured up to 300 kOe for the amorphous alloys are slightly larger than those of the quasicrystalline alloys, and the paramagnetic Curie temperature of the former alloys is larger than that of the latter alloys. The magnitude of effective magnetic moment P_{eff} determined from the Curie-Weiss law for crystalline alloys is qualitatively explained in terms of the Pauling valence. The value of P_{eff} of the quasicrystalline alloys is almost the same as that of the amorphous ones and about two times that of the crystalline alloys at the same composition. From the magnetic measurements it becomes clear that Mn sites are partly magnetic, and the magnetic properties are drastically modified by substituting some fraction of Mn for other transition metals such as Cr. The spin-glass behavior is observed and the spin freezing temperature lies on the same line as a function of Mn content for both the amorphous and quasicrystalline alloys.

The electrical resistivity of the quasicrystalline alloys with a relatively high Mn content is extremely large accompanying a negative temperature coefficient as that of the amorphous alloys. After crystallization, its magnitude is reduced drastically and the temperature dependence curves of the alloys with high concentrations show a positive curvature in the wide temperature range. Therefore, the magnitude and the temperature dependence of electrical resistivity of the quasicrystal-

* The 1845th report of Institute for Materials Research.

** Concurrent address; Institute for Materials Research, Tohoku University.

*** The Institute for Solid State Physics, The University of Tokyo.

line alloys are very different from those of the crystalline alloys. From these results, it is concluded that the magnetic and electrical properties of Al-Mn quasicrystalline alloys are very similar to those of amorphous ones and distinctly different from those of the crystalline alloys.

1. Introduction

For many decades it has been considered that fivefold axes of symmetry cannot be present in crystals. However, recently, it has been confirmed that a rapidly quenched Al-Mn alloy exhibits single crystal-like sharp electron diffraction spots with an icosahedral point symmetry, and the alloys having such characteristics is termed "quasicrystal". It has become clear that the three-dimensional Penrose tiling is able to construct a non-periodic lattice with a perfect long-range icosahedral order. On the other hand, mathematical models based on the Landau theory with icosahedral point symmetry and quasiperiodic translational order have been also proposed in order to explain the structure of quasicrystals¹⁾. Since the discovery of Al-Mn quasicrystals, a number of Al-transition metal quasicrystalline alloys have been found. The physical properties of these quasicrystalline alloys have been investigated¹⁾ by many workers. Especially structural studies have been carried out extensively¹⁾.

The concentration dependence of the effective magnetic moment of Al-Mn quasicrystalline, amorphous and crystalline alloys has been investigated²⁻⁷⁾. The spin-glass behavior and the extremely high electrical resistivity of Al-Mn quasicrystalline and amorphous alloys have been confirmed²⁻⁷⁾. Furthermore, the logT dependence of electrical resistivity at low temperatures for Al-Mn quasicrystalline and amorphous alloys has been demonstrated⁸⁾.

In the present review, the following magnetic and electrical properties of Al-Mn quasicrystalline alloys will be discussed and compared with those of amorphous and crystalline counterparts because the amorphous structure is often correlated with the icosahedral structure. The magnetic properties of Mn and its alloys and compounds are significantly affected by the environment of Mn atoms. In order to verify the relationship between the magnetic moment and the Pauling valence⁹⁾, the magnetic properties of several kinds of Al-Mn and Al-Mn-Si crystals will also be presented.

- a) Magnetic Moment and Paramagnetic Curie Temperature
- b) Pauling Valence vs. Magnetic Moment
- c) Spin Glass Behavior
- d) Electrical Resistivity and Magnetoresistance

2. Experimental

Various kinds of Al-Mn and Al-Mn-Si crystalline compounds, and four kinds of Al-Mn alloy targets were prepared by arc-melting in an argon atmosphere using starting materials of Al of 99.99, Si of 99.999 and Mn of 99.9 wt% in purities. The melting was repeated five times. The amorphous alloys were prepared by dc sputtering on a water-cooled Cu disk covered with a Capton. Their amorphous state was confirmed by X-ray diffraction using Cu-K $_{\alpha}$ radiation. The alloy compositions of Mn and Al were determined by spectropotometry and titration methods, respectively.

The magnetization curve up to 70 kOe at 4.2 K and the temperature dependence of magnetization at a strength of 20 kOe from 4.2 K to 90 K were obtained by an extraction method using a superconducting magnet. The temperature dependence of the ac susceptibility was measured in a magnetic field of 10 Oe with a frequency of 200 Hz. The magnetic cooling was carried out in 370 Oe and the temperature dependence of the dc susceptibility was measured in the same magnetic field. The magnetization curves were also measured at 4.2 K using an induction method in pulsed high magnetic fields up to 300 kOe with a duration of 13 ms¹⁰⁾. The measurement of electrical resistivity was carried out from 4.2 K to room temperature by a conventional four-terminal method.

3. Results and discussion

a) Magnetic Moment and Paramagnetic Curie Temperature

The magnetization curves at 4.2 K up to 70 kOe for Al-Mn quasicrystalline alloys are shown in Fig.1(a), together with those of four kinds of Al-Mn amorphous alloys in Fig.1(b), and with those of three kinds of Al-Mn crystalline ones in Fig.1(c)^{3,4,6)}. As seen from these figures, the magnetizations of the quasicrystalline and amorphous alloys are similar in the magnitude and much larger than those of crystalline alloys.

Figure 2(a) shows the temperature dependence of the dc susceptibility of Al-Mn quasicrystalline alloys. These curves exhibit a very similar behavior of Al-Mn amorphous alloys as seen from Fig.2(b). That is, the temperature dependence curves show a Curie-Weiss type variation. The inverse susceptibility of these alloys, however, does not show a straight line as shown in Fig.3. Then, the Curie constant C was deduced from the following equation by assuming a temperature independent susceptibility term χ_0 ;

$$\chi - \chi_0 = C / (T - \theta_p) \quad (1),$$

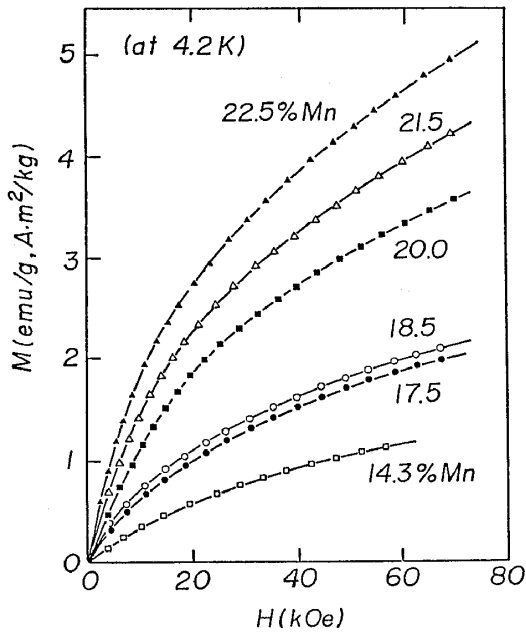


Fig.1(a). Magnetization curves of Al-Mn quasicrystalline alloys.

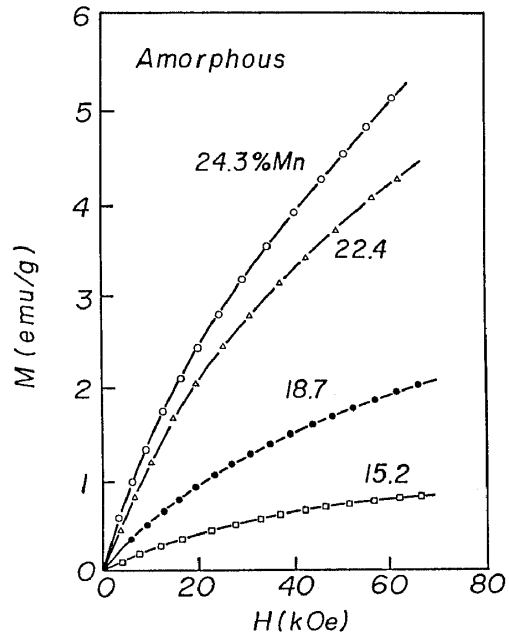


Fig.1(b). Magnetization curves of Al-Mn amorphous alloys.

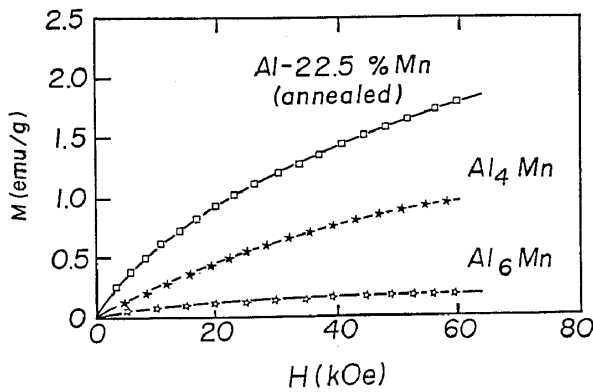


Fig.1(c). Magnetization curves of Al-Mn crystalline alloys.

where θ_p is the paramagnetic Curie temperature. Figure 3 illustrates the susceptibility and its inverse susceptibility of $Al_{77.5}Mn_{22.5}$ quasicrystalline alloy. As shown in the figure, θ_p exhibits a negative value associated with a negative exchange interaction. From the constant value of C , the effective magnetic moment P_{eff} is deduced. Figure 4 shows the concentration dependence of P_{eff} of Al-Mn quasicrystalline alloys, together with that of Al-Mn amorphous and crystalline alloys^{4,6}. There are some problem

in the fitting with Eq.(1) for the quasicrystalline alloys. The samples with low Mn content below 20% are observed to contain a small amount of crystalline an Al phase by X-ray diffraction²⁾. On the other hand, a decagonal phase is slightly induced in the specimen with high Mn content above 20%^{11,12)}. The present data, however,

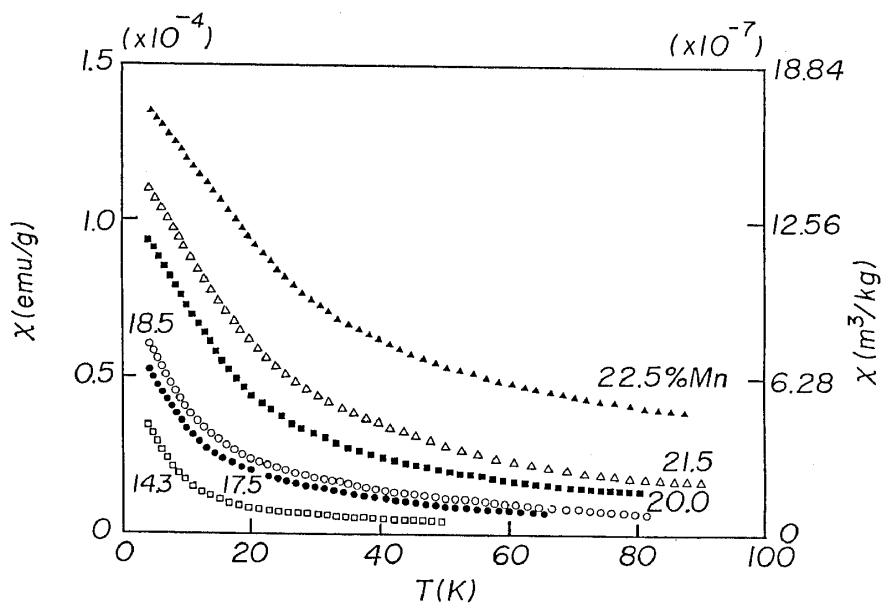


Fig.2(a). Temperature dependence of the susceptibility of several kinds of Al-Mn quasicrystalline alloys.

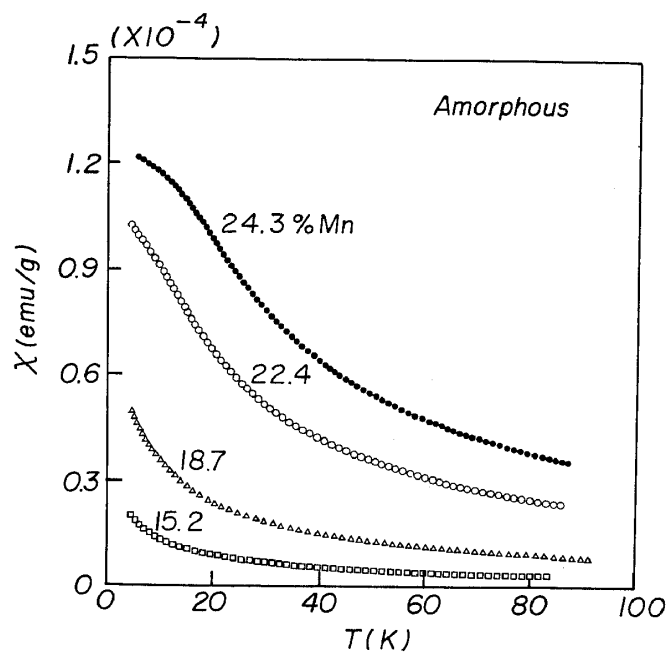


Fig.2(b). Temperature dependence of the susceptibility of four kinds of Al-Mn amorphous alloys.

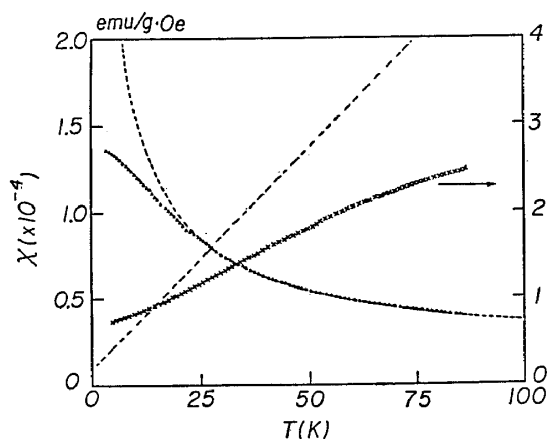


Fig.3. Temperature dependence of susceptibility and inverse susceptibility of Al_{77.5}Mn_{22.5} alloy.

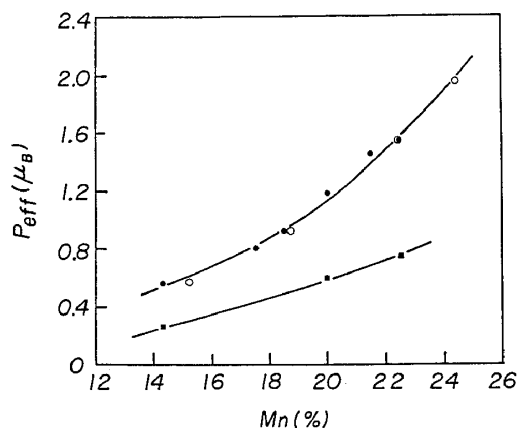


Fig.4. Concentration dependence of effective magnetic moment of Al-Mn alloy system.

have been conventionally analyzed using Eq.(1), because the ratio of Al or decagonal phase is very small, being minor in the following discussions. The values of the quasicrystalline alloys are very similar to those of the amorphous alloys and much larger than those of crystalline alloys. That is, in the wide composition range, the values of the former two alloy systems are about twice that of crystalline alloys. The concentration dependence of the paramagnetic Curie temperature θ_p of Al-Mn amorphous and quasicrystalline alloys is shown in Fig. 5. The values of the latter alloys are somewhat ambiguous in the low concentration of Mn because these alloys contain a small amount of Al phase dissolved several percent of Mn¹³⁾. However, there is a distinct difference between the amorphous and quasicrystalline

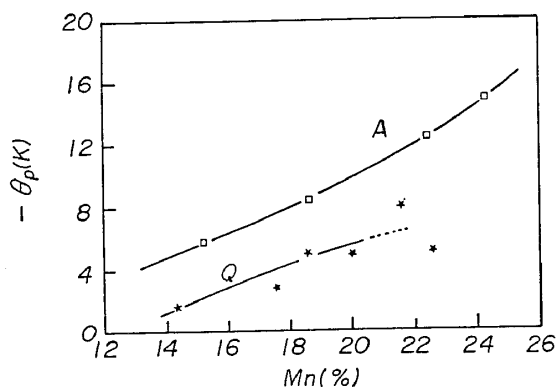


Fig.5. Concentration dependence of the paramagnetic Curie temperature of Al-Mn alloy system.

alloys, that is, the values of the former alloys are much larger than those of the latter alloys, suggesting that the average Mn-Mn interactions are weakly antiferromagnetic and the interaction of the former is stronger than that of the latter, although the magnitude of the effective magnetic moment is practically equal to each other as shown in Fig. 4.

The average local magnetic moment per Mn atom, $\langle \mu \rangle$, which corresponds to the saturation magnetization is deduced from the Curie constant by assuming $g = 2$ with the following expression;

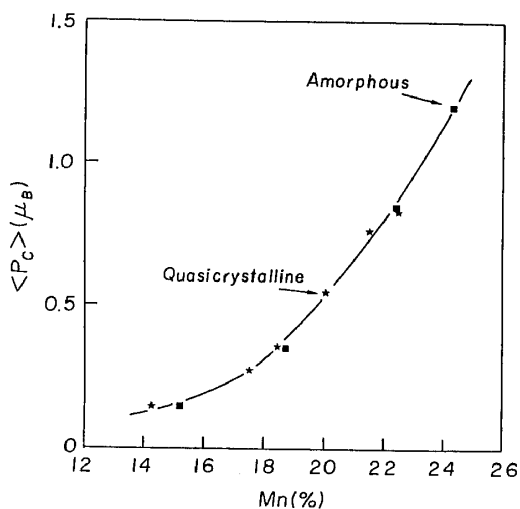


Fig.6. Concentration dependence of the average local magnetic moment per Mn atom.

$$C = N \mu_B^2 \langle P_c \rangle (\langle P_c \rangle + 2) / 3k_B \quad (2),$$

where N is the number of Mn atoms, μ_B the Bohr magnetron and k_B the Boltzmann constant. In Fig.6, the values of $\langle P_c \rangle$ for the quasicrystalline alloys and amorphous alloys are plotted as a function of Mn content. The magnitude of the average local moment for the quasicrystalline alloy with 20 % Mn is consistent with the value estimated from the effective Bohr magneton number reported by other authors^{12,14}.

Figures 7(a) and (b) show the magnetization curves of Al-Mn quasicrystalline and amorphous alloys at 4.2 K in pulsed high magnetic fields up to 300 kOe⁵. These curves coincide well with those obtained in the steady fields up to 70 kOe^{3,4}. All M-H curves are convex upward and such a tendency is more pronounced as Mn concentration decreases, then the curve of Al_{85.7}Mn_{14.3} quasicrystalline alloy is almost saturated at 300 kOe. However, it becomes difficult to saturate the magnetization even at 300 kOe with increasing Mn content. These magnetization processes are quite similar to those of a typical spin

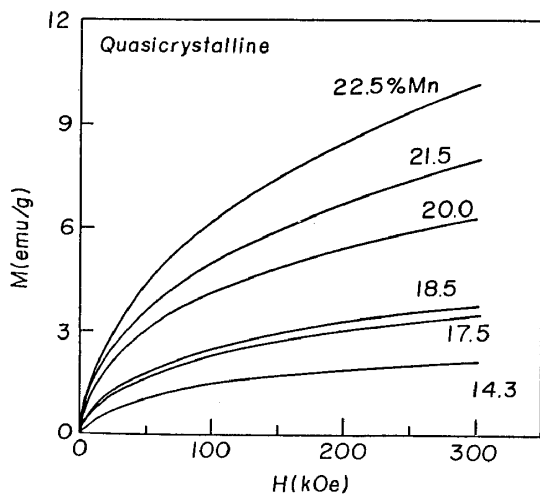


Fig.7(a). Magnetization curves up to 300 kOe for Al-Mn quasicrystalline alloys.

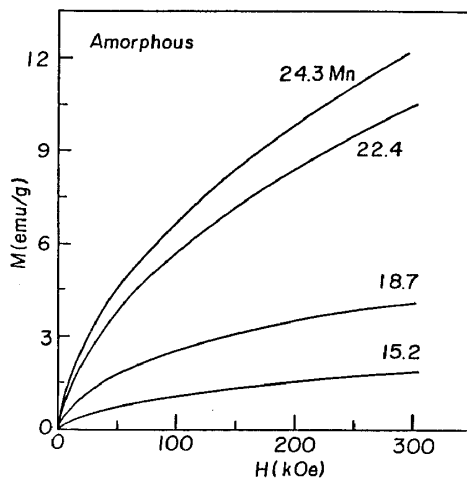


Fig.7(b). Magnetization curves up to 300 kOe for some Al-Mn amorphous alloys.

glass system with competing exchange interactions such as Cu-Mn alloys¹⁵⁾. Actually, a spin glass behavior has been recognized in the Al-Mn quasicrystalline alloys as well as in the amorphous alloys (see Figs.13 and 14).

Magnetic properties of Al-Mn quasicrystalline alloys are very similar to those of amorphous alloys mentioned above, but we can see a slight difference of the magnetization process in the same concentration alloys between both states. Figure 8

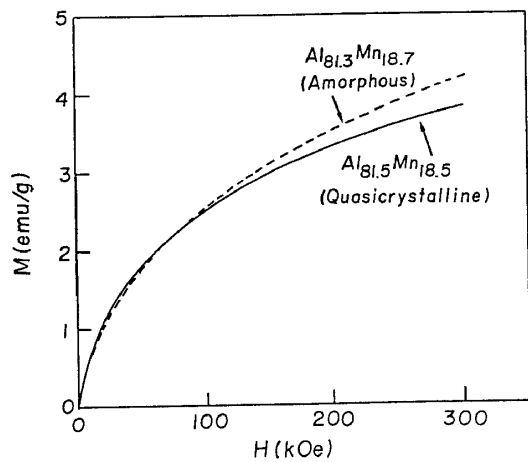


Fig.8. Magnetization curves of Al-Mn quasicrystalline and amorphous alloys.

shows the magnetization processes of Al_{81.3}Mn_{18.7} amorphous alloy and that of Al_{81.5}Mn_{18.5} quasicrystalline alloy. The saturation of magnetization of the former is more difficult than that of the latter. The concentration dependence of the average saturation magnetization per Mn, M_s , estimated from the magnetization curves is presented in Fig.9, which is in harmony with that of the average local moment, $\langle \mu \rangle$, deduced from the susceptibility measurements as shown in Fig.6, but the values of M_s are much smaller than those of $\langle \mu \rangle$ in both phases. This fact implies that the number of magnetic sites are smaller than that of Mn sites in both

phases because the number of magnetic sites is assumed to be equal to that of Mn sites in the estimation of $\langle \mu \rangle$. Using the values of the Curie constant, C , and the saturation magnetization per Mn atom, M_s , we can evaluate the atomic fraction, X_m , and the average local moment, P_c , of the magnetic sites in the Al-Mn alloys from the following relations;

$$M_s \left(\frac{M_s X_m}{X_s} + 2 \mu_B \right) = 3k_B C/N \quad (3),$$

$$P_c = \frac{M_s X_m}{X_s} \mu_B \quad (4),$$

where the g factor is assumed to be 2. Figure 10 shows the values of X_m in the quasicrystalline and amorphous phases. It should be emphasized that the number of magnetic sites is very small compared with that of the Mn sites in both phases. In the Al_{85.7}Mn_{14.3} quasicrystalline alloy, the magnetic site is only 0.9 at%. The atomic fraction of magnetic sites increases to about 2.5 % in the Al₈₀Mn₂₀ quasicrystalline alloy. The number of magnetic sites in the amorphous phase is slightly larger than that in the quasicrystalline phase. Warren et al. have estimated the atomic fraction of nonmagnetic Mn sites in Al-Mn quasicrystalline alloys

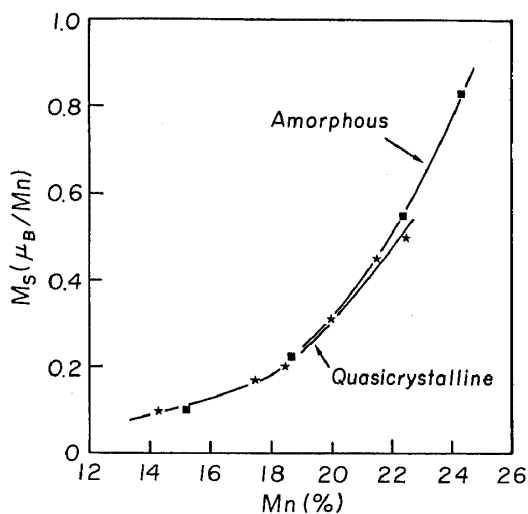


Fig.9. Concentration dependence of the average saturation magnetization per Mn of Al-Mn alloy system.

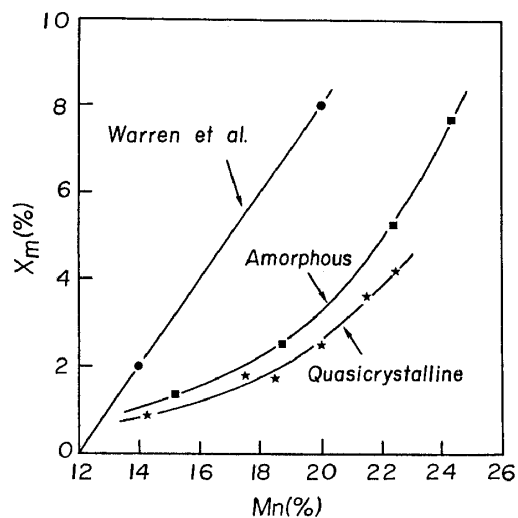


Fig.10. Concentration dependence of the atomic fraction of Mn having a magnetic moment.

using NMR spin-echo techniques. The estimated value was a roughly constant 12% in the Mn concentration range between 14 and 20 %¹⁶⁾. The atomic fraction of magnetic sites obtained from the NMR data are also shown in the same figure for comparison. These values are much larger than those of the present results. In the NMR experiment, the nonmagnetic fraction can be evaluated from the relative intensity of the ^{55}Mn and ^{27}Al contributions to the spin-echo spectra, because the observed ^{55}Mn NMR signal is derived only from the nonmagnetic sites. The resonance signals from the magnetic sites are expected to be unobservably broad due to the localized electron spin fluctuations¹⁶⁾. It should be noted that the NMR spin-echo techniques underestimate the number of nonmagnetic Mn sites when the resonances of some nonmagnetic sites are broadened unobservably by broad electric field gradient distributions and by hyperfine fields from the local moments of the remaining magnetic sites. The number of these unobservable nonmagnetic sites will increase with increasing Mn content. In this situation, the atomic fraction of magnetic sites estimated from the NMR experiments would be considered to become larger than that from the high-field measurements.

The experimental results of Mossbauer effect for Al(MnFe) quasicrystalline alloys have also suggested that two distinct transition metal sites are present in these alloys^{17,18)}. On the other hand, a continuous distribution of sites in AlCuFe quasicrystalline alloy has been reported¹⁹⁾ and the distribution curve of the quadrupole splitting is similar to that of amorphous alloy²⁰⁾. In the lower Mn concentration range, therefore, some Mn sites will be occupied by Al atoms or the occupation probabilities of Al atoms at some Al sites will increase in the

quasicrystalline alloy. These effects reduce the atomic fraction of magnetic Mn sites in the quasicrystalline alloy because the magnitude of each Mn moment is significantly influenced by its environment, that is, its nearest neighbor atoms and the atomic distance, as discussed in the succeeding section. The atomic fraction of magnetic sites will also decrease in the amorphous phase with decreasing Mn content by the same reason, because the local atomic structure of the quasicrystalline phase is very similar to that of the amorphous phase, that is, the pair distribution functions in the quasicrystalline and amorphous phases are similar up to the second nearest-neighbors²¹⁾. As is well known, a two-dimensional quasiperiodic structure has been described by Penrose²²⁾. A three-dimensional Penrose tiling can be achieved with rhombohedral oblate and prolate assembled within respect of matching rules^{23,24)}. The resulting structure is non-periodic but is perfectly ordered in the long distance. A three dimensional Penrose tiling gives sharp diffraction spots whose distribution obeys the rules of the icosahedral point group symmetries when Fourier transformed into reciprocal space. Setting the experimental diffraction intensities against the calculated values, it is considered that Mn atoms are mainly present on the vertices of a three dimensional Penrose tiling while Al atoms are located on the faces of both rhombohedra and on the triad axis of the prolate rhombo-

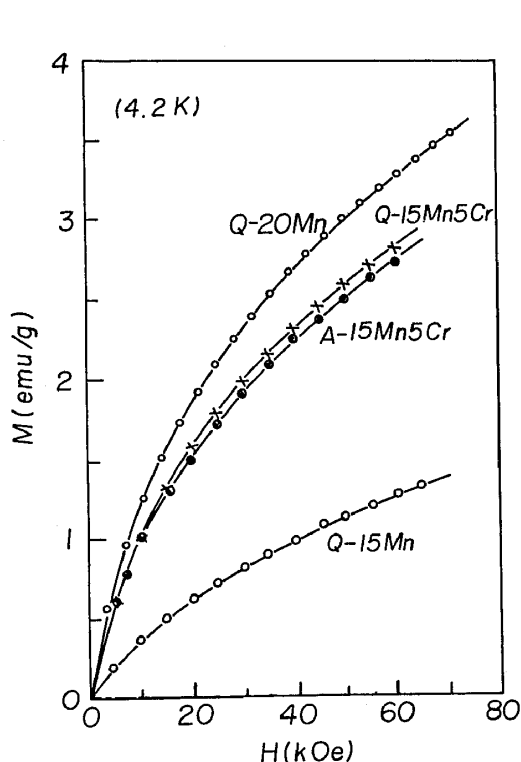


Fig.11. Magnetization curves of Al-Mn and Al-Mn-Cr alloys.

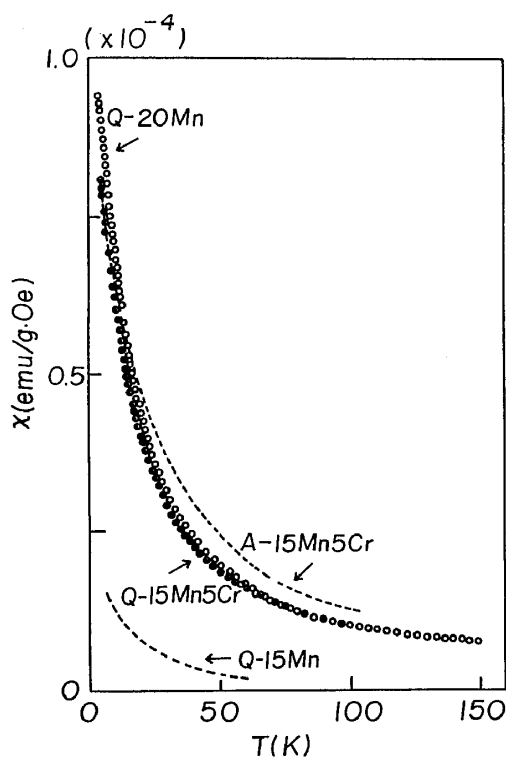


Fig.12. Temperature dependence of the susceptibility of Al-Mn-(Cr).

hedra²⁴⁾. As shown in Fig.10, there are Mn sites with and without magnetic moment. The preferential substitution of Mn sites by other transition metals such as Fe and V have been discussed, and suggested²⁵⁾ that the size of the substitutional element is a possible of the site preference.

Figure 11 shows the magnetization curves up to 70 kOe for Al-Mn-Cr quasicrystalline alloys, together with that of Al₈₀Mn₁₅Cr₅ amorphous alloy. The magnetization of Al₈₀Mn₁₅Cr₅ quasicrystalline alloy is comparable to that of the amorphous counterpart. It should be noted that these two values are much larger than that of Al₈₅Mn₁₅ quasicrystalline alloy. Figure 12 shows the temperature dependence of susceptibility of these alloys. The effective magnetic moments deduced from Eq.(1) for the former two alloys are about twice that of the latter alloy. Therefore, the average effective Mn moment is drastically enhanced by addition of Cr having no magnetic moment in such a low concentration range. Recently, Al-Cu-TM(Transition Metals) quasicrystalline alloys have been developed by Tsai et al.²⁶⁾ In this series, the substitution of transition metals is very easy and various kinds of alloys systems are available, compared with Al-Mn alloy system. The magnetic properties show a systematic trend, depending on the atomic size of substitutional element²⁷⁾. The high-field measurement of AlMnCr and AlCuTM alloy systems would give more detailed information.

b) Pauling Valence vs. Magnetic Moment

The magnitude of magnetic moment of many alloys and compounds containing Mn is related to the atomic distance and the coordination number of atoms. The values of a number of crystalline compounds have been explained²⁸⁾ by using the concept of the Pauling valence⁹⁾. According to Pauling's empirical expression, the atomic distance $D(n)$ is given by

$$D(n) = D(1) - 0.60 \ln 10 \cdot n_o \quad (5),$$

where $D(1)$ is the bond length for a single bond and n the number of bonds. The value of n_o is defined by the following relation;

$$n_o = P.V./C.N. \quad (6),$$

where C.N. is the coordination number and P.V. the Pauling valence which is the number of electrons related to the bonding, and given by the following expression for individual site of Mn atom by²⁷⁾

$$(P.V.)_{ij} = \sum (C.N.)_{ij} \exp \left[\frac{D(1) - D(n_o)_{ij}}{0.26} \right] \quad (7).$$

In order to confirm the validity of this expression, the values of P.V. of several kinds of Al-Mn and Al-Mn-Si crystalline alloys have been calculated. The detailed structure of Al₆Mn alloy has been investigated and the coordination number C.N. and the atomic distance have been reported²⁹⁾. The value of P.V. is obtained from these data by using the single bond radii of Al = 1.248 and Mn = 1.171 Å. As shown in Table 1, the value of P.V. is calculated to be 6.1. On the other hand, α-AlMnSi (cubic, Al_{72.5}Mn_{17.4}Si_{10.1}) crystal structure is closely related to the structure of the icosahedral AlMnSi alloys^{30,31)}. It has been reported that the magnetic properties of Al-Mn-Si amorphous alloys are similar to that of Al-Mn-Si icosahedral alloys¹²⁾. The crystal structure of α-AlMnSi has been determined³²⁾. This phase is composed of 138 atoms in the cubic unit cell with the lattice constant a = 12.68 Å and the space group pm3. The coordination number and the atomic distance have been given without distinction between the two kind light atoms of Al and Si. As shown in Table 1, the Pauling valences P.V. of Mn(1) and Mn(2) are 5.13 and 6.04, respectively. Therefore, the mean value of P.V. is calculated to be 5.56. In the same

Table-1. Pauling valence, coordination number and effective magnetic moment of Al-Mn and Al-Mn-Si alloys.

	Al ₆ Mn	φ-Al ₁₀ Mn ₃	δ-Al ₁₁ Mn ₄	α-Al ₉ Mn ₂ Si _{1.8}	β-Al ₉ Mn ₃ Si
Mn(%)	14.3	23.1	26.7	17.4	23.1
P.V.	6.1	4.7	5.2	5.6	5.7
C.N.	10	8	Mn(1) 12 Mn(2) 12	Mn(1) 10 Mn(2) 9	10
P _{eff} (μ _B)	0.56	1.28	0.63	0	1.09

way, the values of other compounds are also given in the same table. It is interesting to note that the Mn content of φ-AlMn³³⁾ is lower than that of δ-AlMn³⁴⁾, but the effective magnetic moment of the former is larger than that of the latter, accompanying the smaller value of the Pauling valence. The difference of P.V. between α-AlMnSi and β-AlMnSi³⁵⁾ is not so large, but the value of magnetic moment is very different from each other. It seems that the detailed structure analysis is necessary to discuss strictly because no individual sites of two kind light atoms have been given in the former alloy³²⁾. It has been demonstrated that the magnetic moment of many crystalline compounds containing Mn decreases linearly with increasing the value of P.V. and becomes almost zero above P.V.=6.5²⁸⁾. Figure 13 shows the

Pauling Valence vs. magnetic moment of several kinds of AlMn and AlMnSi crystalline alloys⁶⁾, together with that of various alloys and compounds containing Mn^{28,36)}, and pure Mn³⁷⁾. It is worth noting that almost all data are situated within the area restricted by the two dotted lines for the values of γ - and α -Mn(I, II, III and IV). From these results, it can be understood that the general trend of the magnitude of magnetic moment is closely correlated with the atomic distance and the coordination number. Eq.(7) also suggests that the covalency effect plays an important role in the change of magnetic moments.

It has been pointed out that the icosahedra should be prevalent in liquids near the melting temperature³⁸⁾ because the icosahedral cluster of 13 atoms has a lower energy compared with that of nuclei of fcc and hcp crystals for Lennard-Jones pair potentials³⁹⁾. Furthermore, electronic structure and magnetic property of Co have been investigated by assuming the icosahedral short range order in amorphous metals and the reasonable results have been obtained⁴⁰⁾. The pair distribution functions of Pd-U-Si alloys in both quasicrystalline and amorphous states have been examined and pointed out that there is no distinct difference up to the second nearest neighbors, or up to 6A²¹⁾. Therefore, it is expected that the amorphous structure is not so different from the icosahedral structure in the short range, resulting in the same magnitude of the effective magnetic moment P_{eff} in the present Al-Mn alloy system.

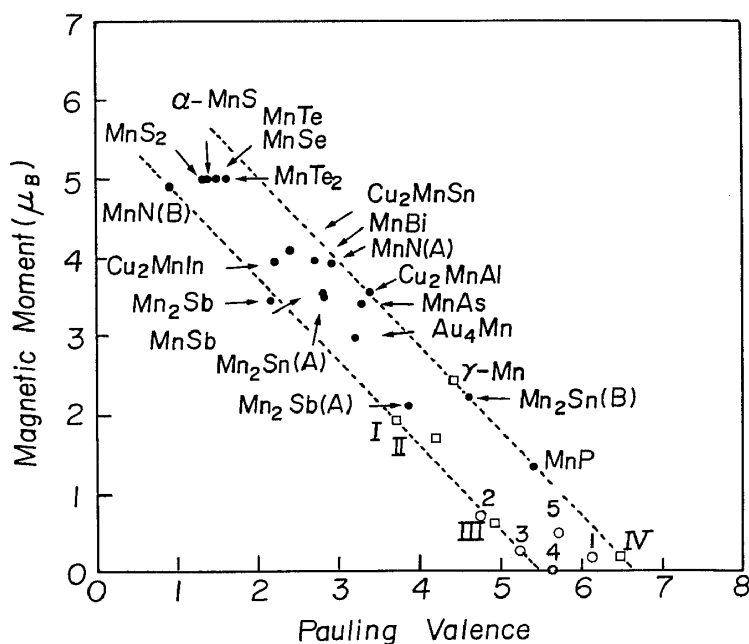


Fig.13. Magnetic moment vs. Pauling valence of various kinds of alloys and compounds containing Mn and pure Mn (1. Al₁₁Mn₄, 2. ϕ -Al₁₀Mn₃, 3. δ -Al₁₁Mn₄, 4. α -Al₉Mn₂Si_{1.8}, 5. β -Al₉Mn₃Si₆).

c) Spin Glass Behavior

As mentioned in connection with Fig.10, most Mn sites are non-magnetic. Furthermore, Mn atoms are hardly to be found as the first nearest-neighbors according to available structure investigations¹⁾. Therefore, Mn atoms act mainly as isolated atoms and we can make up a physical picture in direct analogy to dilute Al-Mn alloys. As is well known, the spin glass behavior is often created by the RKKY interaction in such dilute alloys. In fact, the spin-glass behavior of Al-Mn quasi-crystalline alloys has been confirmed^{3,4,12)}. As shown in Figs. 14(a) and (b), the

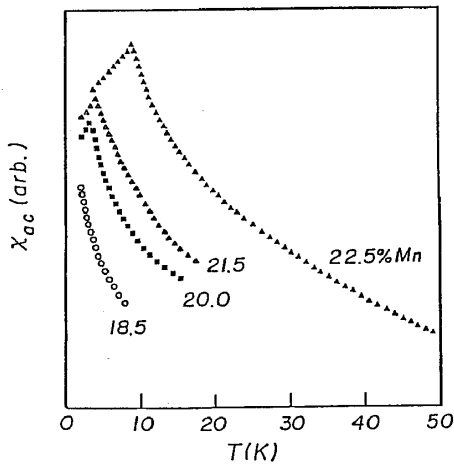


Fig.14(a). Temperature dependence of ac susceptibility of Al-Mn quasi-crystalline alloys.

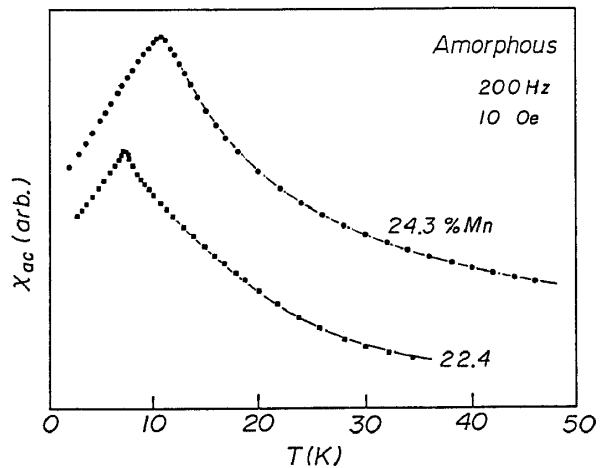


Fig.14(b). Temperature dependence of ac susceptibility of Al-Mn amorphous alloys.

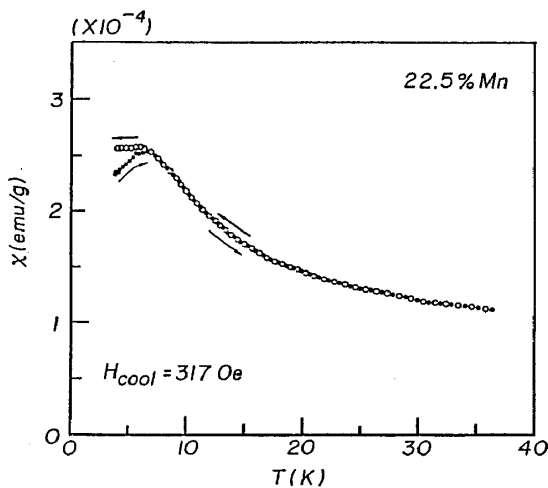


Fig.15. Magnetic cooling effect of $Al_{77.5}Mn_{22.5}$ alloy.

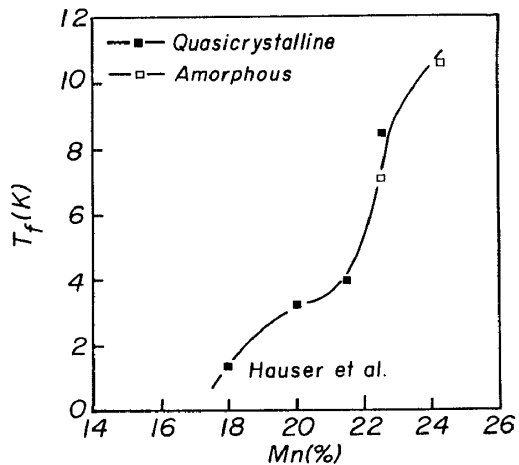


Fig.16. Concentration dependence of the spin freezing temperature.

temperature dependence of ac susceptibility of Al-Mn quasicrystalline and amorphous alloys exhibits a distinct cusp in the low temperature range. The magnetic cooling effect of $\text{Al}_{75.5}\text{Mn}_{24.5}$ quenched alloy has been examined. The dc susceptibility curve shows a hysteresis after magnetic cooling in the magnetic strength of 317 Oe as shown in Fig.15⁴⁾. From the results of Figs.14 and 15, it is concluded that the Al-Mn quasicrystalline and amorphous alloys also show the spin-glass behavior at low temperatures. Figure 16 shows the concentration dependence of the spin freezing temperature T_f in the quasicrystalline phase, together with that in the amorphous phase for Al-Mn alloy system³⁾. The

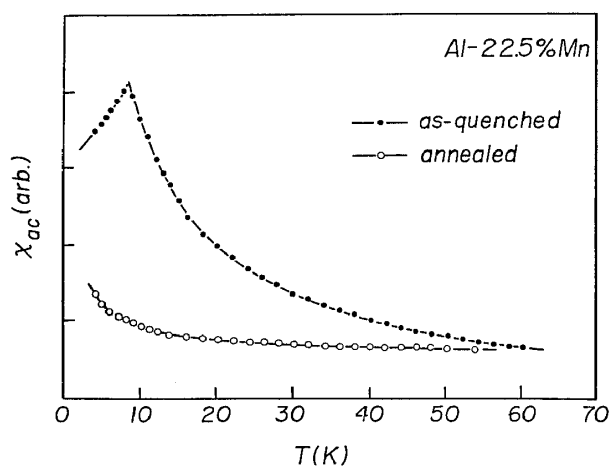


Fig.17. Temperature dependence of ac susceptibility of $\text{Al}_{77.5}\text{Mn}_{22.5}$ alloys.

is also shown in the same figure. These experimental data are on the same line without making no distinction each other. Therefore, the similar behavior of magnetic property between the amorphous and the quasicrystalline states is confirmed again. Figure 17 shows the temperature dependence of the ac susceptibility for $\text{Al}_{77.5}\text{Mn}_{22.5}$ quenched and annealed alloys. By annealing, the spin glass behavior is eliminated and the magnetic moment is drastically reduced, being comparable to that of $\text{Al}_{85.7}\text{Mn}_{14.3}$ quasicrystalline alloy.

d) Electrical Resistivity and Magnetoresistance

The temperature dependence of electrical resistivity ρ of Al-Mn quasicrystalline alloys is shown in Fig.18. With increasing Mn content, the value of ρ drastically increases and the remarkable temperature dependence with a negative temperature coefficient is observed at low temperatures in the high Mn content alloys, being analogous to that of amorphous alloys with the similar Mn content as shown in Fig.19.⁶⁾ The high electrical resistivity of amorphous alloys is attributed to the short mean-free-path due to the non-periodicity in the amorphous structure. However, the contribution from only the non-periodicity would not result in such a high electrical resistivity of $\text{Al}_{75.7}\text{Mn}_{24.3}$ amorphous alloy. Because $\text{Al}_{66.7}\text{Y}_{33.3}$ amorphous alloy exhibits the value $\rho \sim 150 \mu\Omega \text{ cm}$, which is very common in amor-

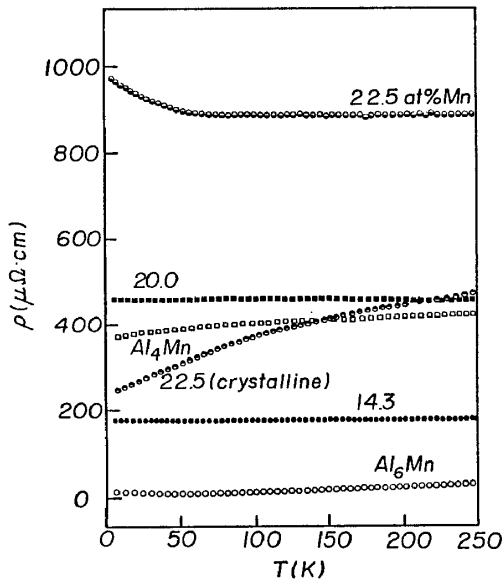


Fig.18. Temperature dependence of electrical resistivity of Al-Mn quasicrystalline and crystalline alloys.

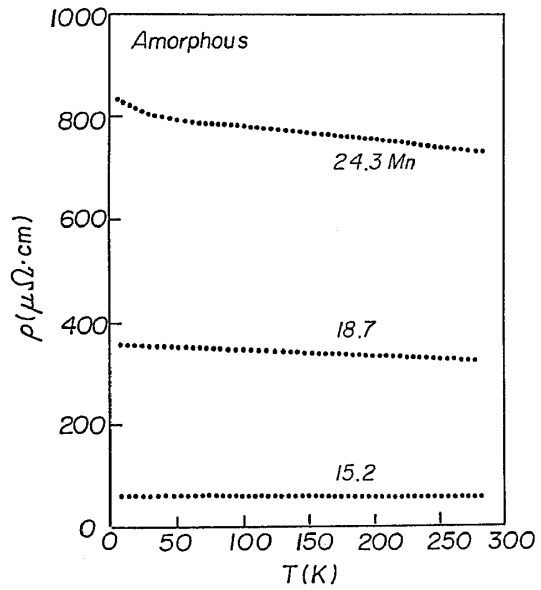


Fig.19. Temperature dependence of electrical resistivity of Al-Mn amorphous alloys.

phous alloys⁴²⁾, other contributions such as the resonant state scattering⁴³⁾ and the magnetic scattering due to the localized moment⁴⁴⁾ would be superimposed. When Mn atoms are dissolved in Al, a resonant state of the Fermi electron with the d-state of Mn should take place because the center of the virtual bound state is very close to the Fermi level⁴³⁾. The contribution of the resonant state to the electrical resistivity of Al-Mn quasicrystalline alloys has been discussed^{3,7,45)}. In the case of Al-Y alloy system mentioned above, the resonant state does not result in a high electrical resistivity because the Fermi level would not so close to the resonant state. Therefore, it is considered that the value of ρ of Al_{66.7}Y_{33.3} amorphous alloy is not so high as reported⁴¹⁾. Furthermore, it is worth noting that the electrical resistivity of Al_{66.7}Gd_{33.3} amorphous alloy⁴¹⁾ is much higher by about three times than that of Al_{66.7}Y_{33.3} amorphous alloy due to the additional contribution from the localized magnetic moment. From these results, it is considered that there are main three contributions to the electrical resistivity and the total value of ρ is give by;

$$\rho = \rho_{dis} + \rho_{res} + \rho_{mag} \quad (8),$$

where ρ_{dis} is the disorder scattering associated with the amorphous structure and does not satisfies the Bloch condition, ρ_{res} the resonant scattering by the virtual

bound state, ρ_{mag} the magnetic scattering due to the localized moment.

Figures 20(a) and(b) show the electrical resistance normalized by the value at 4.2 K as a function of logarithmic scale of temperature for $\text{Al}_{77.5}\text{Mn}_{22.5}$ quasicrystalline and $\text{Al}_{75.7}^{\text{mag}}\text{Mn}_{24.3}$ amorphous alloy, respectively. The magnetic field was applied perpendicularly to the current. The linear relationship is not held below T_f and the negative magnetoresistance is observed below this temperature. These characteristic behaviors are found to be the same within the experimental accuracy when the field is applied along the current. The change of slope has been obtained in the amorphous alloy as shown in Fig.20(b). The temperature dependence at low temperatures is closely correlated with the spin freezing in both quasicrystalline and amorphous alloys, that is, the slope of $-\log T$ plot clearly changes at the spin freezing temperature T_f (see Fig.16). Therefore, the temperature dependence of electrical resistivity should take into account the magnetic contribution. The low temperature enhancement of resistivity in these Al-Mn alloys is one or two order of magnitude stronger than that of non-magnetic amorphous alloys⁴⁶⁾. This fact leads to the minor effect of the weak Anderson localization in the bulk disordered state of Al-Mn alloys. The outlines of the electrical properties common to both quasicrystalline and amorphous phases are summarized as follows;

- Above T_f , the temperature dependence obeys $-\log T$,
- Below T_f , the weaker dependence than $-\log T$ is observed,
- Below T_f , the negative magnetoresistance appears. Its magnitude is enhanced on cooling and tends to saturate with the $\log H$ dependence.

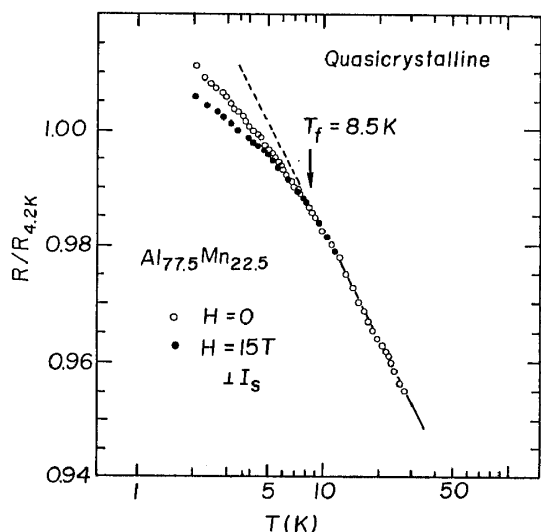


Fig.20(a). Electrical resistance at $H = 0$ and 15T for $\text{Al}_{77.5}\text{Mn}_{22.5}$ quasicrystalline alloy.

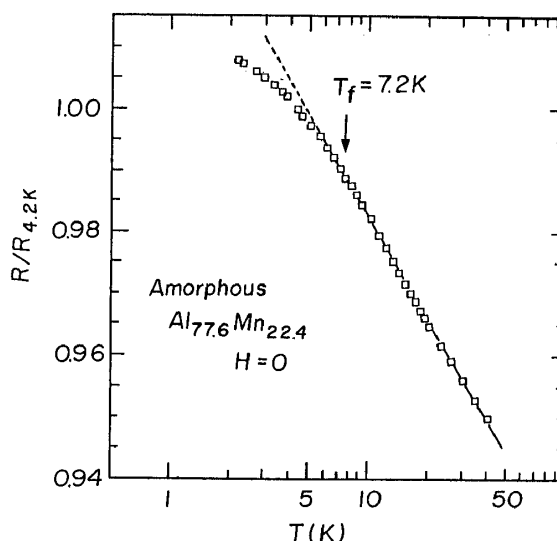


Fig.20(b). Electrical resistance at $H = 0$ for $\text{Al}_{77.6}\text{Mn}_{22.4}$ amorphous alloy.

By heating at the rate of 10 K/min, the amorphous alloys transform at first into the crystalline and quasicrystalline alloys, and finally the quasicrystalline phase does into the crystalline phase. The magnitude of ρ and its temperature dependence are drastically changed after crystallization by annealing as seen from Fig.18^{3,7)}.

The magnetic and electrical properties of Al-Mn alloys in the quasicrystalline, amorphous and crystalline states have been discussed in this review and it becomes clear that almost all properties in the quasicrystalline and amorphous states are similar but different from those in the crystalline state. It should be noted that the comparison of Pd-U-Si alloys in three states leads to a similar conclusion. That is, the electronic, transport and magnetic properties in the quasicrystalline and amorphous states are very similar but different from those in the crystalline state⁴⁷⁾.

4. Conclusion

Al-Mn and Al-Mn-Si crystalline compounds, and Al-Mn amorphous alloys were prepared by arc-melting and sputtering, respectively, in order to compare the magnetic and electrical properties in the amorphous, quasicrystalline and crystalline Al-Mn states. It is concluded that these properties of the quasicrystalline alloys are very similar to those of the amorphous alloys and are very different from those of crystalline alloys. The main results are summarized as follows:

1) The magnetization of the amorphous alloys is slightly large compared with that of the quasicrystalline alloys. The paramagnetic Curie temperature of the former alloys is larger than that of the latter alloys.

2) The effective magnetic moment P_{eff} of the quasicrystalline alloys is almost same as that of the amorphous ones, but it is much larger than that of the crystalline alloys, being about twice.

3) From the magnetic measurements, it becomes clear that there are different Mn sites in quasicrystalline and amorphous phases, that is, the magnetic and non-magnetic sites and the part of the former is very small.

4) The magnitude of magnetic moment of Al-Mn and Al-Mn-Si crystalline alloys tends to be explained by the Pauling valence which takes into account the atomic distance and the coordination number.

5) The magnetic properties of Al-Mn quasicrystalline and amorphous alloys are drastically modified by substitution of some part of Mn for other transition metals.

6). The temperature dependence of the ac susceptibility in the quasicrystalline state shows a distinct cusp at low temperatures and the dc hysteresis curve

due to the magnetic cooling effect is confirmed. These data are closely correlated with the spin-glass behavior in a similar as the amorphous alloys composed of the similar Mn content.

7). The spin freezing temperature T_f in the quasicrystalline state increases with increasing Mn content and the concentration dependence of T_f is on the same line of that for the amorphous alloys.

8). The electrical resistivity ρ in the quasicrystalline phase increases with the increase of Mn content, and the temperature dependence and the magnitude of are comparable with those of the amorphous alloys having the similar composition of Mn. The magnitude of electrical resistivity would be accounted quantitatively by three contributions, namely, the structural disorder scattering, magnetic scattering and the resonant scattering.

9) The negative magnetoresistance of $\text{Al}_{77.5}\text{Mn}_{22.5}$ quasicrystalline alloy becomes larger with decreasing temperature and tends to saturate with increasing magnetic field.

10) After crystallization by annealing, the magnitude of electrical resistivity is drastically reduced, showing the positive temperature coefficient.

Acknowledgments

The authors would like to thank Prof. T. Masumoto, Prof. A. Inoue, Prof. N. Toyota and Mr. H. M. Kimura of Institute for Materials Research, Tohoku University, and Dr. Sakakibara and Mr. S. Todo of the Institute for Solid State Physics, The University of Tokyo, who participated in much of the study discussed in the present paper, for many illuminating discussions. The sputtering amorphous samples were prepared at the laboratory of Prof. H. Fujimori of Institute for Materials Research. The authors wish to thank Mr. M. Hosoya and his co-workers of Institute for Materials Research for chemical analysis of the sputtered amorphous specimens. Grateful acknowledgment is made to Mr. H. Komatsu for the magnetic measurements.

The present work was supported by Grad-in-Aid for Scientific Project from the Ministry of Education, Japan.

References

- 1) Introduction to Quasicrystals, ed by M.V. Jaric (Academic Press Inc., 1988).
- 2) T. Masumoto, A. Inoue, M. Oguchi, K. Fukamichi, K. Hiraga, M. Hirabayashi: Trans. JIM, 27(1986), 81.

- 3) K. Fukamichi, T. Masumoto, M. Oguchi, A. Inoue, T. Goto, T. Sakakibara and S. Todo: J. Phys., F16(1986), 1059.
- 4) K. Fukamichi, T. Goto, T. Masumoto, T. Sakakibara, M. Oguchi and S. Todo: J. Phys. F, 17(1987), 743.
- 5) T. Goto, T. Sakakibara and K. Fukamichi: J. Phys. Soc. Jpn., 57(1988), 1751.
- 6) K. Fukamichi and T. Goto, to be submitted.
- 7) K. Fukamichi, M. Oguchi, H. Kimura and T. Masumoto: Sci. Rep. RITU, A33(1986), 211.
- 8) N. Toyota, K. Fukamichi, A. Inoue, K. Matsuzaki and T. Masumoto: J. Phys. Soc. Jpn., 57(1988), 1726.
- 9) L. Pauling: The Nature of the Chemical Bond(1960), New York, Cornell University Press, P.221-64.
- 10) N. Yamada, S. Takeyama, T. Sakakibara, T. Goto and N. Miura: Phys. Rev., B34(1986), 4121.
- 11) L. Bendersky, R.J. Schaefer, F.S. Biancaniello, W.J. Boettinger, M.J. Kaufman and D. Shechtman: Scripta Met., 19(1985), 909.
- 12) J. J. Hauser, H.S. Chen and J.V. Waszczak: Phys. Rev., B33(1986), 3577.
- 13) A. Inoue, L. Arnberg, B. Lehtinen, M. Oguchi and T. Masumoto: 1986, Met. Trans., 17A(1986), 1657.
- 14) F.L.A. Machado, W.G. Clark, L.J. Azevedo, D. Yang, W.A. Hines, J.I. Budnick and M.X. Quan: Solid State Commun., 61(1987), 145.
- 15) J.J. Smith, G.J. Nieuwenkuys and L.J. de Jongh: Solid State Commun., 31(1979), 265.
- 16) W.W. Warren, H.S. Chen and G.P. Espinosa: Phys. Rev., B34(1986), 4902.
- 17) L.J. Swartzendruber, S. Shechtman, L. Bendersky and J.W. Cahn: Phys. Rev., B32(1985), 1383.
- 18) R.A. Dunlap, D.W. Lawther and D.J. Lloyd: Phys. Rev., B38(1988), 3649.
- 19) Z.M. Stadnik and G. Stroink: Phys. Rev., B38(1988), 10447.
- 20) N. Kataoka, A.P. Tsai, A. Inoue, T. Masumoto and Y. Nakamura: Jpn. J. Appl. Phys., 27(1988), L1125.
- 21) D.D. Kofalt, S. Nanao, T. Egami, K.M. Wong and S.J. Poon: Phys. Rev. Lett., 57(1986), 114.
- 22) R. Penrose: Bull. Inst. Math., 10(1974), 266.
- 23) T. Ogawa: J. Phys. Soc. Jpn., 54(1985), 3205.
- 24) C. Janot and J.M. Dubois: J. Non-cryst. Solids, 106(1988), 193.
- 25) K. Kimura, H. Yamane, S. Takeuchi, K. Koga, T. Shimizu and H. Yasuoka: MRS Sympo. Proc., in press.
- 26) A.P. Tsai, A. Inoue and T. Masumoto: Jpn. J. Appl. Phys., 26(1987), L1505.
- 27) K. Fukamichi, T. Goto, H. Komatsu, H. Wakabayashi, A.P. Tsai, A. Inoue and T. Masumoto: ICM (Paris,1988), in press.

- 28) N. Mori and T. Mitsui: J. Phys. Soc. Jpn., 25(1968), 82.
- 29) A.D.I. Nicol: Acta Crystallogr., 20(1953), 285.
- 30) V. Elser and C.L. Henley: Phys. Rev. Lett., 26(1985), 2883.
- 31) D.C. Koskenmaki, H.S. Chen and K.V. Rao: Phys. Rev. B33(1986), 5328.
- 32) M. Cooper and K. Robinson: Acta Cryst., 20(1966), 614.
- 33) M.A. Taylor: Acta Cryst., 12(1959), 393.
- 34) J.B. Bland: Acta Cryst., 11(1958), 236.
- 35) K. Robinson: Acta Cryst., 5(1952), 397.
- 36) Handbook on the Magnetic Substances(Asakura Co. Ltd., 1975), in Japanese.
- 37) T. Yamada, N. Kunitomi, Y. Nakai, D.E. Cox and G. Shirane: J. Phys. Soc. Jpn., 28(1970), 615.
- 38) D.R. Nelson: Phys. Rev., B28(1983), 5515.
- 39) F.C. Frank: 1952, Proc. Roy. Soc., A215(1952), 43.
- 40) M.E. McHenry, M.E. Eberhart, R.C. O'Handley and K.H. Johnson: Phys. Rev. Lett., 56(1986), 81.
- 41) K. Moorjani and J.M.D. Coey: Magnetic Glasses(Elsevier Pub., 1984), p. 197.
- 42) K.V. Rao: Amorphous Metallic Alloys(Butterworths Co. Ltd., 1983), p.401.
- 43) J. Friedel: Canad. J. Phys., 34(1956), 1190.
- 44) T. Kasuya: Prog. Theor. Phys., 16(1956), 45
- 45) C. Berger, D. Pavuna, F. Cyrot-Lackmann and M. Cyrot: Mat. Sci. Eng., 99(1988), 353.
- 46) U. Mizutani: Prog. Matter. Sci., 28(1983), 97.
- 47) P. Grutter, H. Bretscher, G. Indlekofer, H. Jenny, R. Larka, P. Oelhafen, R. Wiesendanger, T. Zingg and H.-J. Guntherodt: Mat. Sci. Eng., 99(1988), 357.